

Mueller matrix measurements and modeling pertaining to Spectralon white reflectance standards

Øyvind Svensen,^{1*} Morten Kildemo,² Jerome Maria,² Jakob J. Stamnes,¹ and Øyvind Frette¹

¹Department of Physics and Technology, University of Bergen, P.O. Box 7803, N-5020 Bergen, Norway

²Department of Physics, NTNU, 7491 Trondheim, Norway

*oyvind.svensen@projectiondesign.com

Abstract: The full Mueller matrix for a Spectralon white reflectance standard was measured in the incidence plane, to obtain the polarization state of the scattered light for different angles of illumination. The experimental setup was a Mueller matrix ellipsometer, by which measurements were performed for scattering angles measured relative to the normal of the Spectralon surface from -90° to 90° sampled at every 2.5° for an illumination wavelength of 532 nm. Previously, the polarization of light scattered from Spectralon white reflectance standards was measured only for four of the elements of the Muller matrix. As in previous investigations, the reflection properties of the Spectralon white reflectance standard was found to be close to those of a Lambertian surface for small scattering and illumination angles. At large scattering and illumination angles, all elements of the Mueller matrix were found to deviate from those of a Lambertian surface. A simple empirical model with only two parameters, was developed, and used to simulate the measured results with fairly good accuracy.

© 2012 Optical Society of America

OCIS codes: (290.5820) Scattering measurements; (290.5855) Scattering, polarization; (290.1350) Backscattering; (290.1990) Diffusion.

References and links

1. "A guide to diffuse reflectance coatings & materials;" [http://www.prolite.co.uk/File/coatings materials documentation.php](http://www.prolite.co.uk/File/coatings%20materials%20documentation.php).
2. "Reflectance standards product sheet 8.pdf" <http://www.labsphere.com/data/userFiles/>.
3. E. A. Early, P. Y. Barnes, B. C. Johnson, J. J. Butler, C. J. Bruegge, S. F. Biggar, P. R. Spyak, and M. M. Pavlov, "Bidirectional reflectance round-robin in support of the Earth observing system program," *Am. Met. Soc.* **17**, 1078–1091 (2000).
4. D. A. Haner, B. T. McGuckin, and C. J. Bruegge, "Polarization characteristics of Spectralon illuminated by coherent light," *Appl. Opt.* **38**(30), 6350–6356 (1999).
5. B. Gordon, "Integrating sphere diffuse reflectance technology for use with UV-Visible spectroscopy;" Tech. Note: 51450, Thermo Fisher Scientific, WI, USA.
6. D. A. Haner, B. T. McGuckin, R. T. Menzies, C. J. Bruegge, and V. Duval, "Directional-hemispherical reflectance for spectralon by integration of its bidirectional reflectance," *Appl. Opt.* **37**(18), 3996–3999 (1998).
7. K. J. Voss and H. Zhang, "Bidirectional reflectance of dry and submerged Labsphere Spectralon plaque," *Appl. Opt.* **45**(30), 7924–7927 (2006).
8. G. T. Georgiev and J. J. Butler, "The effect of incident light polarization on Spectralon BRDF measurements," *Proc. SPIE* **5570**, 492–502 (2004).
9. AA. Bhandari, B. Hamre, Ø. Frette, L. Zhao, J. J. Stamnes, and M. Kildemo, "Bidirectional reflectance distribution function of Spectralon white reflectance standard illuminated by incoherent unpolarized and plane-polarized light," *Appl. Opt.* **50**(16), 2431–2442 (2011).
10. G. T. Georgiev and J. J. Butler, "The effect of speckle on BRDF measurements," *Proc. SPIE* **588**, 588203 (2005).
11. B. T. McGuckin, D. A. Haner, R. T. Menzies, C. Esproles, and A. M. Brothers, "Directional reflectance characterization facility and measurement methodology," *Appl. Opt.* **35**(24), 4827–4834 (1996).

12. M. Chami, "Importance of the polarization in the retrieval of oceanic constituents from the remote sensing reflectance," *J. Geophys. Res.* **112**(C5), 5026–5039 (2007).
13. G. D. Gilbert and J. C. Pernicka, "Improvement of underwater visibility by reduction of backscatter with a circular polarization technique," *Appl. Opt.* **6**(4), 741–746 (1967).
14. G. Yao, "Differential optical polarization imaging in turbid media with different embedded objects," *Opt. Commun.* **241**(4-6), 255–261 (2004).
15. G. W. Kattawar and D. J. Gray, "Mueller matrix imaging of targets in turbid media: effect of the volume scattering function," *Appl. Opt.* **42**(36), 7225–7230 (2003).
16. P. W. Zhai, G. W. Kattawar, and P. Yang, "Mueller matrix imaging of targets under an air-sea interface," *Appl. Opt.* **48**(2), 250–260 (2009).
17. J. S. Tyo, D. L. Goldstein, D. B. Chenault, and J. A. Shaw, "Review of passive imaging polarimetry for remote sensing applications," *Appl. Opt.* **45**(22), 5453–5469 (2006).
18. F. Stabo-Eeg, M. Kildemo, I. S. Nerbø, and M. Lindgren, "Well-conditioned multiple laser Mueller matrix ellipsometer," *Opt. Eng.* **47**(7), 073604 (2008).
19. P. S. Hauge, R. H. Muller, and C. G. Smith, "Conventions and formulas for using the Mueller-Stokes calculus in ellipsometry," *Surf. Sci.* **96**(1-3), 81–107 (1980).
20. R. Ossikovski, M. Anastasiadou, S. Ben Hatit, E. Garcia-Caurel, and A. De Martino, "Depolarising Mueller matrices: how to decompose them?" *Phys. Status Solidi* **205**(4), 720–727 (2008).
21. R. Ossikovski, "Interpretation of nondepolarizing Mueller matrices based on singular-value decomposition," *J. Opt. Soc. Am. A* **25**(2), 473–482 (2008).
22. J. J. Gil and E. Bernabeu, "Depolarization and polarization indices of an optical system," *Opt. Acta (Lond.)* **33**(2), 185–189 (1986).
23. F. Le Roy-Bréhonnet, B. Le Jeune, P. Eliés, J. Cariou, and J. Lotrain, "Optical media and target characterization by Mueller matrix decomposition," *Appl. Phys. (Berl.)* **29**, 34–38 (1996).

Introduction

For calibration of optical instruments the availability of a white Lambertian surface, which appears equally bright from all directions regardless of illumination direction and wavelength, would be desirable. Since a white Lambertian surface is not available, a Spectralon white reflectance standard, which is the commercial product closest to a Lambertian surface, is commonly used for calibration purposes. Spectralon is a white diffuse material (based on polytetrafluoroethylene) with excellent reflection properties, produced by Labsphere, USA. It is formed as a thermoplastic resin by heat and pressure treatment, and can be shaped into a variety of shapes. Spectralon has the highest diffuse reflectance values of any known substance (up to 99%) in the ultraviolet (UV), visible (VIS), and near-infrared (NIR) spectral ranges [1, 2], and the reflection properties are spectrally flat between 400 and 1,500 nm. Also, the Spectralon material is thermally stable to above 350 °C, chemically inert, and extremely hydrophobic, and is therefore used in a wide variety of applications as diffuse reflectance standards [3, 4]. It is also used as interiors of integrating spheres, which are reflectance accessories [5] for the creation of diffuse light sources.

In previous studies, Spectralon white reflectance standards were found to behave closely as a Lambertian surface for small scattering and illumination angles, but to deviate from it for large scattering and illumination angles. Haner et al. [6] conducted hemispherical reflectance measurements with VIS and NIR light, and found the total reflectance of Spectralon to be 0.971 ± 0.04 . Voss et al. [7] found the Spectralon reflection properties to be nearly Lambertian for normally incident un-polarized light, Early et al. [3] found them to depend on the illumination and observation angles, and others found them to be polarization dependent [8, 9]. A reoccurring problem in these experiments was the presence of speckles in the measured signal when using a coherent laser as a light source. Georgiev et al. [10] and McGuckin et al. [11] discussed the effect of speckles, as well as methods for reducing such interference effects.

For un-polarized and linearly polarized illumination Spectralon white reflectance standards are well documented and often used as calibration standards, but for applications involving other polarization states more documentation is needed. Imaging polarimetry is a technique used in many fields, such as remote sensing, atmospheric science, and industrial monitoring. It enhances the information available in such imaging applications, but depends on accurate knowledge of the polarization states. Chami [12] found polarization

measurements to be of interest for separating the fraction of inorganic particles from biogenic cells in remote sensing applications. Gilbert et al. [13] applied a circular polarization approach to improve the contrast in underwater visibility. In 2004, Yao [14] developed a Monte Carlo modeling technique to study subsurface polarization imaging of scattering media, and obtained results indicating that different objects appear differently in polarization sensitive imaging. Kattawar et al. [15] found the diagonal elements of the Mueller matrix to be sensitive to perturbations in the environment surrounding the target. Recently, Zhai et al. [16] investigated the use of Mueller matrix imaging beneath an air-sea interface, and found the elements M_{22} and M_{44} to be less influenced by the interface than the other elements. Tyo et al. [17] provided a review of passive imaging polarimetry for remote sensing and found a need for improved calibration techniques in imaging polarimetry.

For these reasons, it is important to measure the full Mueller matrix of Spectralon white reflectance standards for all polarization states. To that end, we used a Mueller matrix ellipsometer (MME) [18] to measure the full Mueller matrix for a Spectralon white reflectance standard pertaining to four different angles of illumination and forward as well as backward observation directions. In these full Mueller matrix measurements, 16 different states of polarization were generated. A polarization state generator (PGS) was used to polarize the incident light in four different states, and a polarization state analyzer (PSA) was used to analyze the scattered light in four different states. Together the PGS and the PSA generated the 16 different elements comprising the full Mueller matrix.

Theory for Mueller matrix of a diffuser

Knowledge of the Mueller matrix allows a complete polarimetric description of light scattered from a partially diffuse object. Here the measurements of the Mueller matrix are based on similar techniques as those used in standard scattering of diffuse, polarized light [4, 9]. But 16 optimally selected intensity measurements were used in order to determine the Mueller matrix with minimum error propagation as described elsewhere [18]. When considering scattering from a surface, it is convenient to refer the polarization states to the plane of incidence in order to obtain the common s and p polarized components. The notation used here for the Stokes vector and Mueller matrix follows the definition given by Hauge et al. [19]. Note that the standard BRDF measurements performed with linear polarizers generating s and p polarized states of the incident light, and analyzing s and p states of the scattered light, are included as a subset of the current measurements of the full Mueller matrix. However, the normalization issues for an absolute BRDF measurement remain as complicated as described in e.g. Bhandari et al. [9].

Several standard Mueller matrices may be considered initially for a partially diffuse sample. The most common form of the Mueller matrix of a general depolarizer is given by [20]:

$$\mathbf{M}_{\Delta}^{ideal} = M_{11} \begin{bmatrix} 1 & 0 & 0 & 0 \\ 0 & a & 0 & 0 \\ 0 & 0 & b & 0 \\ 0 & 0 & 0 & c \end{bmatrix}. \quad (1)$$

A Lambertian surface, is a homogenous, isotropic diffuser with $a = b = c = 0$. For a general non-isotropic diffuser, the diagonal elements a , b , and c in Eq. (1) are positive and less than 1. On the other hand, a non-depolarizing Mueller matrix can be made up of the basic building blocks of the so-called isotropic dichroic retarder, commonly encountered in specular reflection from an isotropic surface [21]:

$$\mathbf{M}_{DR} = M_{11} \begin{bmatrix} 1 & m_{21} & 0 & 0 \\ m_{12} & m_{22} & 0 & 0 \\ 0 & 0 & m_{33} & m_{34} \\ 0 & 0 & m_{43} & m_{44} \end{bmatrix}. \quad (2)$$

In the special case of reflection from an isotropic surface, $m_{12} = m_{21} = -\cos(2\psi)$, $m_{33} = m_{44} = \sin(2\psi)\cos(\Delta)$, and $m_{43} = -m_{34} = -\sin(2\psi)\sin(\Delta)$. Here ψ and Δ are the commonly defined ellipsometric parameters $R_p/R_s = \tan\psi e^{i\Delta}$ [21], where R_p and R_s are the reflection coefficients for the s and p components, respectively.

In previous studies of Spectralon diffusers [8, 9], only linear polarizers in p and s directions were used in the characterization, and hence only the elements M_{11} , M_{12} , M_{21} , and M_{22} were measured. All other elements were disregarded, but it was noted that the Mueller matrix must be of the form:

$$\mathbf{M}_{\Delta}^{\text{ideal}} = \begin{bmatrix} M_{11} & M_{12} & ? & ? \\ M_{21} & M_{22} & ? & ? \\ ? & ? & ? & ? \\ ? & ? & ? & ? \end{bmatrix}, \quad (3)$$

where M_{11} for small illumination and scattering angles is much larger than either of $|M_{12}|$, $|M_{21}|$, and $|M_{22}|$. However, $|M_{12}|$, $|M_{21}|$, and $|M_{22}|$ would increase significantly for large scattering and illumination angles. In this work, the aim is to understand the significance of the Mueller matrix elements denoted by question marks in Eq. (3) for a Spectralon diffuser used as a reference standard. To that end, the full Mueller matrix pertaining to four different illumination angles $\theta_0 = 0^\circ, 30^\circ, 45^\circ$, and 60° was measured for scattering angles θ between 0° and 180° for every 2.5° . Earlier measurements showed that speckle effects from laser light would influence BRDF measurements [10, 11]. To reduce speckle effects a rotating diffuser was inserted in front of the polarization optics. One full Mueller matrix measurement to obtain the 16 different elements of the Mueller matrix in addition to one dark measurement for each element took about 50 seconds. During each full measurement stability was required. This was achieved using an ultra-stable laser and a stable photomultiplier detector, thus providing reasonably good absolute measurements also of the scattering phase function M_{11} , which depends both on the illumination angle θ_0 and the scattering angle θ .

Results and discussion

An interesting feature that may be studied in detail whenever the complete Mueller matrix is available is the so-called depolarization index p (or degree of purity), which is obtained from the full Mueller matrix as follows [22, 23]:

$$p = \left(\frac{\left(\text{tr}(\mathbf{M}^t \mathbf{M}) - M_{11}^2 \right)}{3M_{11}^2} \right)^{\frac{1}{2}} = \left(\frac{\left(\left(\sum_{i,j=1}^4 M_{i,j}^2 \right) - M_{11}^2 \right)}{3M_{11}^2} \right)^{\frac{1}{2}}. \quad (4)$$

The depolarization index is between 0 and 1, i.e. $0 \leq p \leq 1$. When $p = 0$, the scattered light is fully depolarized, as it would be for scattering from a Lambertian surface, and when $p = 1$, the scattered light is fully polarized. The left-hand side in Fig. 1 shows that a simple empirical model (to be described below) can be used to simulate the depolarization index that is

obtained from Eq. (4) and the measured results for the Mueller matrix. For small scattering angles (θ), the depolarization index is seen to be very small (regardless of the value of the illumination angle (θ_0)), but as θ and θ_0 increase, p increases, as would be expected since then many of the elements of the Mueller matrix differ from zero. Note that all other common forms of the linear depolarization index previously reported [4, 9], can be readily produced from the Mueller matrix, as it completely describes the transformation of any incident polarization state.

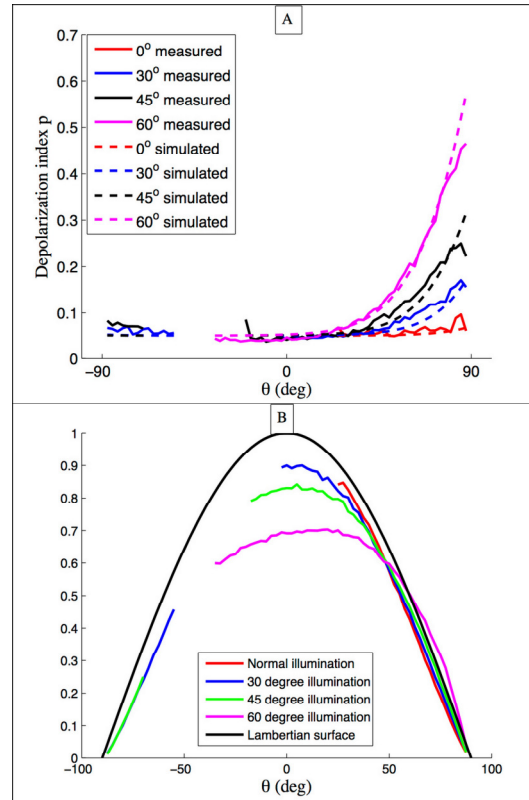


Fig. 1. A: Depolarization index p for simulated and measured results. B: M_{11} element for a Lambertian surface (with depolarization index $p = 0$) and measured for a Spectralon surface with illumination at normal incidence ($\theta_0 = 0^\circ$), as well as for $\theta_0 = 30^\circ$, $\theta_0 = 45^\circ$, and $\theta_0 = 60^\circ$. The y-axis is normalized to the Lambertian surface.

On the right-hand side in Fig. 1, the M_{11} element (representing the scattering phase function) is shown for the same four illumination angles as in the left-hand side of the figure. For a Lambertian surface, M_{11} would be independent of the illumination angle θ_0 , and thus only depend on the scattering angle θ , as indicated by the black curve on the right-hand side of Fig. 1.

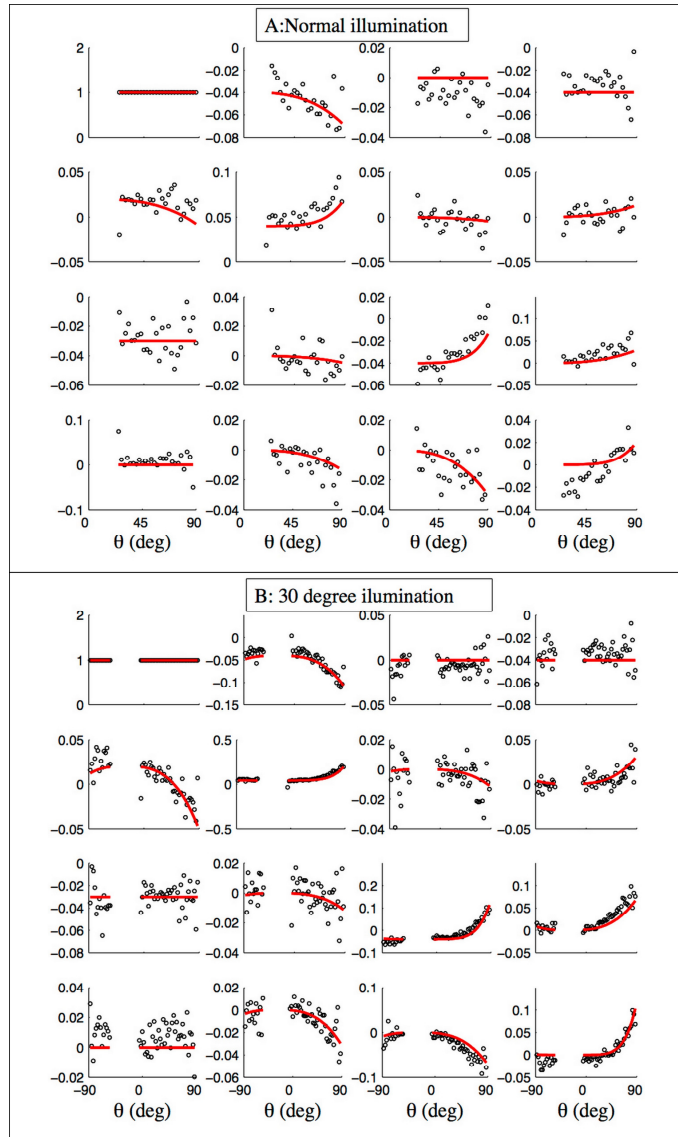


Fig. 2. Measured (black) and simulated (red) normalized Mueller matrices for four different illumination angles θ_0 . A: Normal incidence ($\theta_0 = 0$). B: $\theta_0 = 30^\circ$. The element M_{11} is the so-called scattering phase function (from particle scattering terminology), normalized to its maximum value. The y-axis is normalized to the m_{22} element.

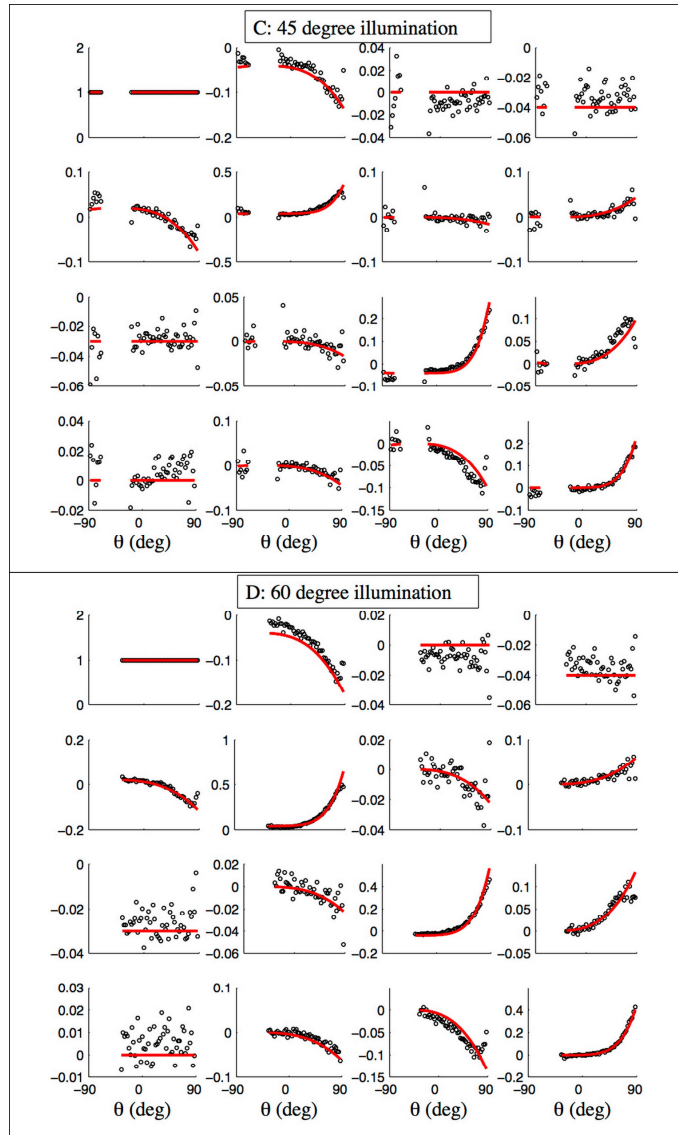


Fig. 3. Measured (black) and simulated (red) normalized Mueller matrices for four different illumination angles θ_0 . C: $\theta_0 = 45^\circ$. D: $\theta_0 = 60^\circ$. The element M_{11} is the so-called scattering phase function (from particle scattering terminology), normalized to its maximum value. The y-axis is normalized to the m_{22} element.

Figure 2 and 3 shows the 16 normalized Mueller matrix elements (black dots) for each of the four illumination angles $\theta_0 = 0^\circ, 30^\circ, 45^\circ,$ and 60° together with simulated results (red curves) based on a simple empirical model to be described below. Many of the elements appear insignificant compared to the noise level in the measurement. A close inspection of the Mueller matrices in Fig. 2 and 3 shows that the most significant elements can be summarized as:

$$\mathbf{M}_{\text{Spectralon}} = M_{11} \begin{bmatrix} 1 & m_{21} & \approx 0 & \approx 0 \\ m_{12} & m_{22} & m_{23} & m_{24} \\ \approx 0 & m_{32} & m_{33} & m_{34} \\ \approx 0 & m_{42} & m_{43} & m_{44} \end{bmatrix}, \quad (5)$$

where each quantity m_{ij} represents a normalized Mueller matrix element. The elements m_{13} , m_{14} , m_{31} , and m_{41} are all constant (within the noise level) for all illumination and scattering angles and less than 0.05.

The absolute value of each normalized element (except M_{11} see Fig. 1), increases with the scattering angle θ , and also with the illumination angle θ_0 . In particular, the normalized diagonal elements m_{22} , m_{33} , and m_{44} increase to 0.5 for $\theta_0 = 60^\circ$ and $\theta = 85^\circ$, indicating that the Spectralon sample to a significant degree behaves like the partial diffuser described by Eq. (1), and hence rather different from a Lambertian diffuser, which is described by Eq. (1) with $a=b=c=0$. However, at small illumination angles θ_0 (less than 30°) and scattering angles less than $|\theta| < 80^\circ$, the Spectralon diffuser behaves to a large extent as a Lambertian diffuser for which each normalized diagonal element m_{22} , m_{33} , or m_{44} is less than 0.05.

Each of the off-diagonal elements m_{12} , m_{21} , m_{43} , or m_{34} is smaller than the diagonal elements by a factor between 2 and 3, but is still significant, particularly at large illumination angles θ_0 (see Fig. 2 and 3). A comparison with Eq. (2) shows that the non-vanishing values of the elements m_{43} and m_{34} indicate the presence of a dichroic retarder component, i.e. scattering where the polarization of the scattered light is not scrambled or lost. As for an isotropic dichroic retarder, there appears to be significant symmetry between elements m_{34} and m_{43} (i.e. $m_{34} \approx m_{43}$) as well as between m_{12} and m_{21} .

The non-vanishing elements m_{23} , m_{32} , m_{42} , and m_{24} (see Fig. 2 and 3), which one also would expect for a rotated dichroic retarder, may be explained by light scattering from surface roughness of low spatial frequency. Furthermore, an apparent symmetry may be observed with $m_{24} \approx m_{42}$, $m_{24} \approx -m_{42}$ and $m_{34} \approx -m_{43}$. As a result, a simplified Mueller matrix for the Spectralon diffuser in the plane of incidence is proposed to be as Eq. (5).

This Mueller matrix still appears to have a rather general form, but because of the symmetry between the measured Muller matrix elements, discussed above, it may be parameterized. Since the symmetry also holds for different illumination angles θ_0 , a simple empirical model with only one parameter [see Eqs. (6) and (7) below] can be derived that gives results that agree fairly well with the measured Muller matrices for all four illumination angles θ_0 and scattering angles θ between -80° and 80° . This empirical model can be split into the sum of two matrices, where the first matrix is that of an ideal isotropic diffuser or Lambertian surface, and the second matrix represents a non-depolarizing surface [19, 22, 23]. Even if the latter approximation does not hold and the second matrix can be further decomposed, the representation given in Eqs. (6) and (7) below is a useful form of the Mueller matrix of the Spectralon, since it includes both the depolarization index p , the ideal isotropic diffuser or Lambertian reflector, represented by the first matrix, and its correction, represented by the second matrix.

$$\mathbf{M}_{\text{Spectralon}} = M_{11} \left((1-p) \begin{bmatrix} 1 & 0 & 0 & 0 \\ 0 & 0 & 0 & 0 \\ 0 & 0 & 0 & 0 \\ 0 & 0 & 0 & 0 \end{bmatrix} + \begin{bmatrix} p & -(p\kappa_2 + \kappa_4) & 0 & -\kappa_4 \\ -(p\kappa_2 - \frac{\kappa_4}{2}) & p^2 + \kappa_4 & -p\kappa_2^2 & p\kappa_2\kappa_3 \\ -\kappa_5 & -p\kappa_2^2 & p^2 - \kappa_4 & p\kappa_2 \\ 0 & -p\kappa_2\kappa_3 & -p\kappa_2 & p^2\kappa_1 \end{bmatrix} \right), \quad (6)$$

where

$$p = \frac{(\theta + \theta_0)^3}{22} - 1. \quad (7)$$

Here θ is the scattering angle, θ_0 is the illumination angle, $\kappa_1 = 0.67$, $\kappa_2 = 0.17$, $\kappa_3 = 0.45$, $\kappa_4 = 0.04$, and $\kappa_5 = 0.03$. Our empirical model in Eqs. (6) and (7) and the values for κ_1 , κ_2 , κ_3 , κ_4 and κ_5 were found by a best fit to the measured results. Figure 1 shows that the empirical model give results for the depolarization index that agree fairly well with those calculated from the measured Muller matrix using Eq. (6) for scattering angles θ between -80° and 80° . For all four illumination angles $\theta_0 = 0^\circ$, 30° , 45° , and 60° , the absolute value of the error between normalized simulated and normalized measured Muller matrix elements are less than 0.03. Since the error between the Mueller matrix elements obtained from the simple empirical model in Eqs. (6) and (7) and the measured Muller matrix elements is small, this model provides a simple way to obtain an estimate of all Mueller matrix for different illumination angles θ_0 and scattering angles θ between -80° and 80° .

Conclusion

The Mueller matrix of a Spectralon white reflectance standard diffuser has been measured in the incidence plane. As in previous investigations, the behavior of the Spectralon white reflectance standard for small scattering and illumination angles was found to be close to that of a Lambertian surface. In previous measurements only the four elements related to the intensity (M_{11}) and to linearly polarized light (m_{12} , m_{21} , and m_{22}) have been investigated. The full Mueller matrix measurements show that for large scattering and illumination angles the significance of many of the other elements increases. In particular, the diagonal elements m_{22} , m_{33} , and m_{44} grow significantly for large scattering and illumination angles. Also, the off-diagonal elements m_{12} , m_{21} , m_{34} , and m_{43} , which are a factor 2-3 times smaller than the diagonal elements, and the elements m_{32} , m_{23} , m_{24} , and m_{42} , which are a factor 6-10 times smaller than the diagonal elements, grow significantly for large scattering and illumination angles. For large scattering and illumination angles many elements of the Mueller matrix were found to be significantly different from zero, implying that the behavior of the Spectralon was not close to that of a Lambertian surface. For simulations of the Muller matrix for Spectralon, a simple empirical model has been derived, which provides an easy way of simulating the Muller matrix elements for different scattering and illumination angles.

Acknowledgment

This work was supported by the Norwegian Research Council, grant number 177567/V30, and "The Norwegian Research Centre for Solar Cell Technology" (project number 193829)".